

Four species neutrino oscillations at ν -Factory: sensitivity and CP-violation

A. Donini^{a1}, M.B. Gavela^{a2}, P. Hernández^{b3} and
S. Rigolin^{a4}

^a*Departamento de Física Teórica C-XI, Facultad de Ciencias, Universidad
Autónoma de Madrid, Cantoblanco, Madrid 28049, Spain*

^b*CERN, 1211 Geneve 23, Switzerland*

Abstract

The prospects of measuring the leptonic angles and CP-odd phases at a *neutrino factory* are discussed in the scenario of three active plus one sterile neutrino. We consider the $\nu_\mu \rightarrow \nu_e$ LSND signal. Its associated large mass difference leads to observable neutrino oscillations at short (~ 1 km) baseline experiments. Sensitivities to the leptonic angles down to 10^{-3} can be easily achieved with a 1 Ton detector. Longer baseline experiments (~ 100 km) with a 1 Kton detector can provide very clean tests of CP-violation especially through tau lepton detection.

Key words: NUFACT99, neutrino, sterile, oscillations, CP-violation.

1 Introduction

Indications in favour of neutrino oscillations have been obtained in both the atmospheric and solar neutrino experiments [1,2,3,4]. The atmospheric neutrino data require $\Delta m_{atm}^2 \sim (0.3 - 7) \times 10^{-3}$ eV² whereas the solar neutrino data prefer either $\Delta m_{sun}^2 \sim 10^{-5} - 10^{-4}$ eV² if interpreted as MSW (matter enhanced) oscillations, or $\sim 10^{-10}$ eV² if the vacuum solution is preferred by nature. The LSND data [5] would indicate a $\nu_\mu \rightarrow \nu_e$ oscillation with a third, very distinct, neutrino mass difference: $\Delta m_{LSND}^2 \sim 0.3 - 1$ eV². The usual three neutrino picture has then to be enlarged to explain the present ensemble of data: four different light neutrino

¹ E-mail donini@daniel.ft.uam.es

² E-mail gavela@garuda.ft.uam.es

³ On leave from Departamento de Física Teórica, Universidad de Valencia. E-mail Pilar.Hernandez@cern.ch

⁴ E-mail rigolin@daniel.ft.uam.es

species are needed. The new light neutrino is usually denoted as sterile [6,7], in it cannot have the standard weak interaction charge in order to comply with the strong bounds on the Z^0 invisible decay width [8].

We derive here convenient parametrizations of the physical mixing angles and CP phases in the case of four neutrino species, and study their experimental signals at the *neutrino factory*¹.

For the sake of illustration, we shall consider as a “reference set-up” the neutrino beams resulting from the decay of $n_\mu = 2 \times 10^{20} \mu^+$ s and/or μ^- s in a straight section of an $E_\mu = 10 - 50$ GeV muon accumulator ring. Muon energies of 40 – 50 GeV are at present under discussion [14] as a convenient goal, as they allow good background rejection [15] and do not preclude the exploration of neutrino signals at lower energies. This is because the number of neutrinos in a given energy bin does not depend on the parent muon energy, while the total number of oscillated and interacted neutrinos increases with E_μ [16]. As the dominant signals are expected to peak at “LSND” distances, most of the parameter space can be explored in experiments at short baseline (SBL) distances of O(1) km and with a very small 1 Ton detector. To optimize the observability of CP-violation asymmetries larger distances (O(10-100) km) and larger detector (1 kTon) are needed.

In section 2 we describe our parametrization. Sections 3 and 4 discuss the experimental sensitivities to angles and CP phases, respectively. We conclude in section 5.

2 Four-Neutrino species

The masses of the four neutrino species can be ordered in two ways, as depicted in Fig.1:

- (1) Three almost degenerate neutrinos, accounting for solar and atmospheric oscillations, separated from the fourth neutrino specie by the LSND mass difference;
- (2) Two almost degenerate neutrino pairs, accounting each for solar and atmospheric oscillations, separated by the LSND mass gap.

We refer to these possibilities respectively as class-I and class-II schemes. Both of them contain a number of sub-classes accounting for all the possible ordering of the neutrino species. It has been shown in [17] that the combined analysis of solar, atmospheric and LSND experiments tends to exclude all class-I schemes. We consider then two possible class-II schemes and choose for definiteness the hierarchycal class-IIB scenario in Fig.1. The lighter pair (1-2) is separated by the solar mass difference

¹ For a detailed analysis of the three family scenario see [9,10,11,12,13].

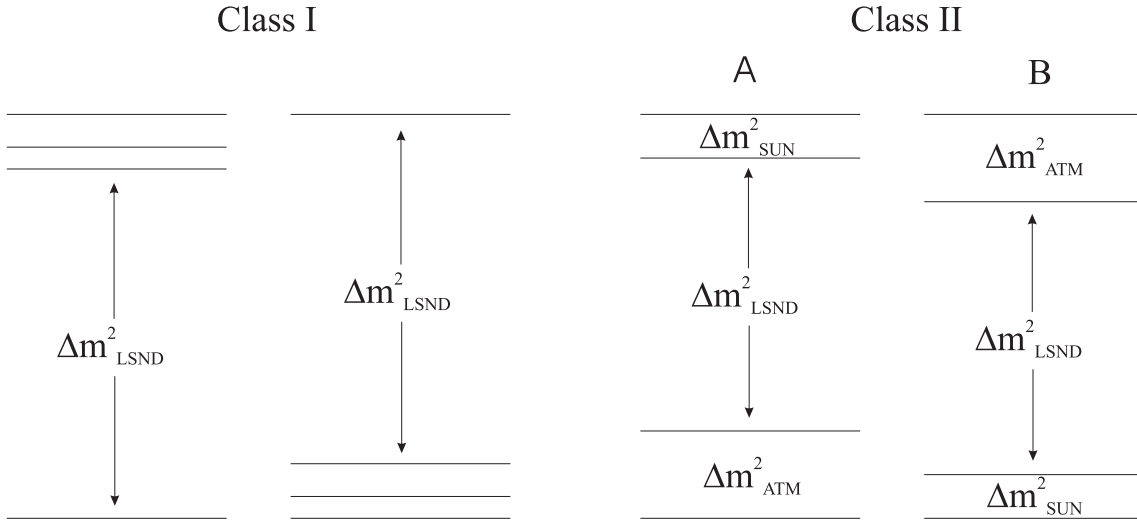


Fig. 1. *Different type of four-neutrino families scenarios: Class-I scenarios (left); Class-II scenarios (right).*

and the heavier pair (3-4) by the atmospheric one². We work in the convention:

$$\nu_s \simeq \nu_1 \leftrightarrow \nu_e \simeq \nu_2 \quad \Delta m_{12}^2 = \Delta m_{sol}^2 \quad (1)$$

with the solar deficit assigned to $\nu_s - \nu_e$ oscillations, and

$$\nu_\mu \simeq \nu_3 \leftrightarrow \nu_\tau \simeq \nu_4 \quad \Delta m_{34}^2 = \Delta m_{atm}^2 \quad (2)$$

with the atmospheric anomaly due to $\nu_\mu - \nu_\tau$ oscillations. The alternative possibility of identifying the atmospheric anomaly as a $\nu_\mu - \nu_s$ oscillation is actually disfavoured by SK data[1].

Whatever the mechanism responsible for neutrino masses, given n light neutrino species oscillation experiments are only sensitive to a unitary $n \times n$ mixing matrix “a la CKM”. In all generality, the parameter space of a four-species scenario would consist of six rotation angles and three complex phases if the neutrinos are Dirac fermions, while it spans six angles plus six phases if the neutrinos are Majorana fermions. Among the latter, three are pure Majorana phases and thus to be disregarded in what follows as they are unobservable in oscillations, reducing the analysis to the mentioned 4×4 “Dirac-type” system.

Within our conventions and the large mass hierarchy indicated by data:

$$\Delta m_{sol}^2 = \Delta m_{12}^2 \ll \Delta m_{atm}^2 = \Delta m_{34}^2 \ll \Delta m_{LSND}^2 = \Delta m_{23}^2, \quad (3)$$

² The alternative option, with a small separation in the heavier pair and a larger one for the lighter pair, amounts to reversing the sign of the LSND mass difference. The analysis below does not depend on this choice.

	Angles	Dirac CP-phases	Majorana CP-phases
Majorana ν 's	6	3	3
Dirac ν 's	6	3	0
Dirac ν 's $\Delta m_{12}^2 = 0$	5	2	0
Dirac ν 's $\Delta m_{12}^2 = \Delta m_{34}^2 = 0$	4	1	0

Table 1

Parameter space for four neutrino families: for Dirac neutrinos we consider the general case with three non-zero mass differences and the particular case (considered in the rest of the paper) with one or two mass differences set to zero; for Majorana neutrinos we consider only the general case.

two approximations are useful:

- (1) $\Delta m_{12}^2 = \Delta m_{34}^2 = 0$, “one mass scale dominance” (or minimal) scheme,
- (2) $\Delta m_{12}^2 = 0$, “two mass scale dominance” (or next-to-minimal) scheme.

The number of independent angles and phases is then reduced as reported in Tab. 1. The minimal scheme is sufficient to illustrate the sensitivity to the mixing angles other than the solar and atmospheric ones. The next-to-minimal scheme is necessary to address the question of CP-violation, as two non-zero mass differences are required to produce observable effects, alike to the standard three-family scenario.

A general rotation in a four dimensional space can be obtained by performing six different rotations U_{ij} in the (i, j) plane, resulting in plenty of different possible parametrizations of the mixing matrix, disregarding phases. We choose the following convenient parametrization, given the hierarchy of mass differences in eq. (3):

$$U = U_{14}(\theta_{14})U_{13}(\theta_{13})U_{24}(\theta_{24})U_{23}(\theta_{23}, \delta_3)U_{34}(\theta_{34}, \delta_2)U_{12}(\theta_{12}, \delta_1). \quad (4)$$

As shown in Table 2, if a given mass difference vanishes the number of physical angles and phases gets reduced by one. A convenient parametrization of the angles is that in which the rotation matrices corresponding to the most degenerate pairs of eigenstates are placed to the extreme right. If the eigenstates i and j are degenerate and the matrix U_{ij} is located to the right in eq. (4), the angle θ_{ij} becomes automatically unphysical. When a different ordering is taken no angle disappears from the oscillation probabilities. A redefinition of the rest of the parameters would then be necessary in order to illustrate the remaining reduced parameter space in a transparent way. Our parametrization corresponds thus to the “cleanest” choice, having settled at the extreme right the rotations corresponding to the most degenerate pairs.

In the ‘‘one mass dominance’’ scheme, the pairs (θ_{12}, δ_1) and (θ_{34}, δ_2) decouple automatically. In the ‘‘two mass dominance’’ scheme, only the pair (θ_{12}, δ_1) does. Thus only the exact number of physical parameters, according to Table 2, remains both in the minimal and next-to-minimal schemes. Notice that it is also important to distribute the phases so that they decouple, together with the angles, when they should.

2.1 Sensitivity reach of the neutrino factory for four neutrino species

We concentrate now on the sensitivity to the different angles in the ‘‘one mass scale’’ approximation, discussed at the beginning of this section. Four rotation angles (θ_{13} , θ_{14} , θ_{23} and θ_{24}) and one complex phase (δ_3) remain. The two rotation angles that have become unphysical are already tested at solar (θ_{12} in our parametrization) and atmospheric (θ_{34}) neutrino experiments. The remaining four can be studied at the *neutrino factory* with high precision, due to the rich flavour content of the neutrino beam. Notice that the number of measurable flavour transitions is enough to constraint them. Consider the following channels:

$$\begin{aligned}
\bar{\nu}_e \rightarrow \bar{\nu}_\mu \rightarrow \mu^+ & \quad (\mu^+ \text{ appearance}) \\
\nu_\mu \rightarrow \nu_\mu \rightarrow \mu^- & \quad (\mu^- \text{ disappearance}) \\
\bar{\nu}_e \rightarrow \bar{\nu}_\tau \rightarrow \tau^+ & \quad (\tau^+ \text{ appearance}) \\
\nu_\mu \rightarrow \nu_\tau \rightarrow \tau^- & \quad (\tau^- \text{ appearance}).
\end{aligned} \tag{5}$$

Separate the CP-even terms, P_{CP} , from the CP-odd ones, $P_{\mathcal{CP}}$, in the following way:

$$P(\nu_\alpha \rightarrow \nu_\beta) = P_{CP}(\nu_\alpha \rightarrow \nu_\beta) + P_{\mathcal{CP}}(\nu_\alpha \rightarrow \nu_\beta). \tag{6}$$

The CP-even parts acquire simple forms:

$$P_{CP}(\nu_e \rightarrow \nu_\mu) = 4c_{13}^2 c_{24}^2 c_{23}^2 s_{23}^2 \sin^2 \left(\frac{\Delta m_{23}^2 L}{4E} \right), \tag{7}$$

$$P_{CP}(\nu_\mu \rightarrow \nu_\mu) = 1 - 4c_{13}^2 c_{23}^2 (s_{23}^2 + s_{13}^2 c_{23}^2) \sin^2 \left(\frac{\Delta m_{23}^2 L}{4E} \right), \tag{8}$$

$$\begin{aligned}
P_{CP}(\nu_e \rightarrow \nu_\tau) = 4c_{23}^2 c_{24}^2 \left[(s_{13}^2 s_{14}^2 s_{23}^2 + c_{14}^2 c_{23}^2 s_{24}^2) \right. \\
\left. - 2c_{14} s_{14} c_{23} s_{23} s_{13} s_{24} \cos \delta_3 \right] \sin^2 \left(\frac{\Delta m_{23}^2 L}{4E} \right),
\end{aligned} \tag{9}$$

$$\begin{aligned}
P_{CP}(\nu_\mu \rightarrow \nu_\tau) = 4c_{13}^2 c_{23}^2 \left[(s_{13}^2 s_{14}^2 c_{23}^2 + c_{14}^2 s_{23}^2 s_{24}^2) \right. \\
\left. + 2c_{14} s_{14} c_{23} s_{23} s_{13} s_{24} \cos \delta_3 \right] \sin^2 \left(\frac{\Delta m_{23}^2 L}{4E} \right).
\end{aligned} \tag{10}$$

Notice that the physical phase appears in $P_{CP}(\nu_e \rightarrow \nu_\tau)$ and $P_{CP}(\nu_\mu \rightarrow \nu_\tau)$ in a pure cosine dependence. Actually, no CP-odd observable can be build out of the oscillation probabilities in this approximation in spite of the existence of a physical CP-odd phase in the mixing matrix.

The existing experimental data impose some constraints on the parameter space, although the allowed region is still quite large. Bugey and Chooz are sensitive to the oscillation $\bar{\nu}_e \rightarrow \bar{\nu}_e$,

$$P(\bar{\nu}_e \rightarrow \bar{\nu}_e) = 1 - 4c_{23}^2 c_{24}^2 (s_{24}^2 + s_{23}^2 c_{24}^2) \sin^2 \left(\frac{\Delta m_{23}^2 L}{4E} \right), \quad (11)$$

resulting in the bound

$$(c_{23}^2 \sin^2 2\theta_{24} + c_{24}^4 \sin^2 2\theta_{23}) \leq 0.2, \quad (12)$$

while Bugey gives a slightly stronger constraint in the larger mass range allowed by LSND. In our computations we safely stay within both experimental constraints. Notice that in the assumption of small angles, this bound forces the mixings s_{23}^2 and s_{24}^2 to be small and leaves more freedom in the mixings of the sterile neutrino: s_{13}^2 and s_{14}^2 .

The allowed mass range for the LSND signal of $\nu_e \rightarrow \nu_\mu$ transitions provides the constraint $10^{-3} \leq c_{13}^2 c_{24}^2 \sin^2 2\theta_{23} \leq 10^{-2}$, which fits nicely with the Chooz constraint to point towards small s_{23}^2 values.

We choose to be “conservative”, or even “pessimistic”, in order to illustrate the potential of the *neutrino factory*. In the numerical computations below we will make the assumption that all angles crossing the large LSND gap, θ_{13} , θ_{14} , θ_{23} and θ_{24} are small.

The large LSND mass difference, $\Delta m_{23}^2 \simeq 1\text{eV}^2$, calls for a SBL experiment rather than a long baseline one. Consider for illustration a 1 Ton detector located at $\simeq 1$ km distance from the neutrino source. We consider a muon beam of $E_\mu = 20$ GeV, resulting in $N_{CC} \simeq 10^7$ charged leptons detected, for a beam intensity of 2×10^{20} useful μ^- per year. An efficiency of $\epsilon_\mu = 0.5, \epsilon_\tau = 0.35$ for μ and τ detection respectively, and a background contamination at the level of $10^{-5} N_{CC}$ events are included.

- θ_{23} and θ_{13} from μ channels

The μ^+ appearance channel is particularly sensitive to θ_{23} . Fig. 2 shows the sensitivity reach in the $s_{23}^2/\Delta m_{23}^2$ plane for different values of θ_{13} . Inside the LSND allowed region the dependence on θ_{13} is mild: s_{23}^2 can reach 10^{-6} for $\theta_{13} \simeq 1^\circ$ or 6×10^{-6} for $\theta_{13} \simeq 60^\circ$.

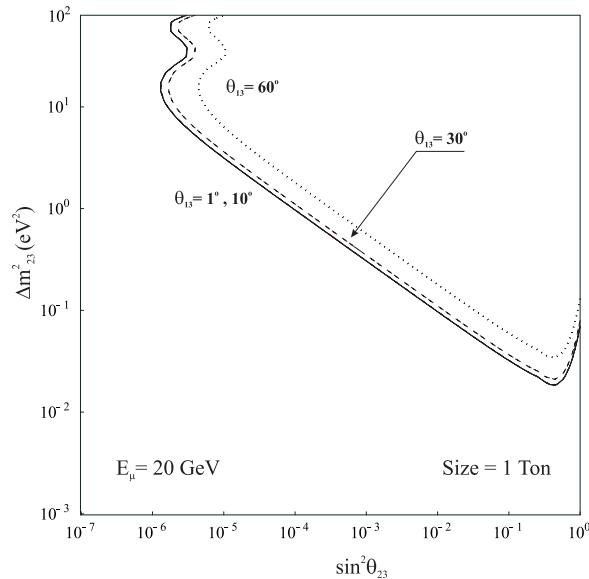


Fig. 2. Sensitivity reach in the $s_{23}^2/\Delta m_{23}^2$ plane at different values of $\theta_{13} = 1^\circ, 10^\circ, 30^\circ$ and 60° for μ^+ appearance. We consider a 1 Ton detector at 1 km from the source and 2×10^{20} useful muons/year.

Concerning the sensitivity to θ_{13} , Fig. 3 (left) illustrates the reach from μ appearance measurements in the $s_{13}^2/\Delta m_{23}^2$ plane, for different values of θ_{23} . Inside the LSND allowed region, the sensitivity to this angle strongly depends on the value of θ_{23} , with the larger sensitivity attained for large values of θ_{23} , a scenario somewhat disfavoured by the LSND measurement. For small values of θ_{23} ($\simeq 1^\circ$), the smallest testable value of s_{13}^2 is $\sim 10^{-2}$. Nevertheless, in this range the muon disappearance channel proves quite more sensitive: in Fig. 3 (right) the sensitivity goes down to values of s_{13}^2 as small as 10^{-4} for $\theta_{23} \simeq 1^\circ$.

- θ_{14} and θ_{24} from τ channels

The τ^- appearance channel is quite sensitive to both s_{14}^2 and s_{24}^2 . Fig. 4 illustrates the sensitivity to s_{14}^2 as a function of θ_{13} : for about 1° , sensitivities of the order of 10^{-2} are attainable, while for 10° the reach extends to 4×10^{-5} . For even larger values of θ_{13} it goes down to 10^{-6} (we recall that θ_{13} is not constrained by the present experimental bounds).

Fig. 5 (left) depicts the foreseeable sensitivity reach to s_{24}^2 as a function of θ_{23} : for small values of θ_{23} the sensitivity to s_{24}^2 goes down to 10^{-6} .

In contrast, the τ^+ appearance channel looks less promising. This is illustrated in Fig. 5 (right): due to the relative negative sign between the two terms in the analytic expression for $P(\nu_e \rightarrow \nu_\tau)$, eq. (9), cancellations for particular values of the angles occur, resulting in a decreasing sensitivity in specific regions of the parameter space. For instance, for $\theta_{23} = 10^\circ$, the reach in s_{24}^2 splits into two separate regions for the LSND allowed range $\Delta m_{23}^2 \sim 10^1$ eV². This sensitivity suppression is absent in the

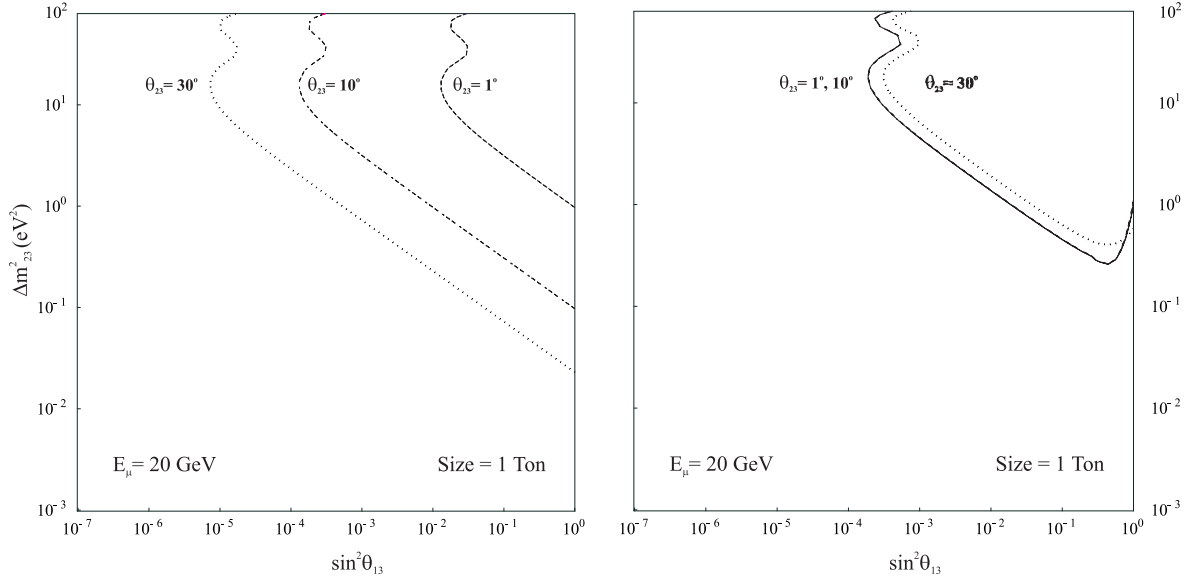


Fig. 3. Sensitivity reach in the $s_{13}^2/\Delta m_{23}^2$ plane at different values of $\theta_{23} = 1^\circ, 10^\circ$ and 30° for μ^+ appearance (left) and disappearance (right). We consider a 1 Ton detector at 1 km from the source and 2×10^{20} useful muons/year.

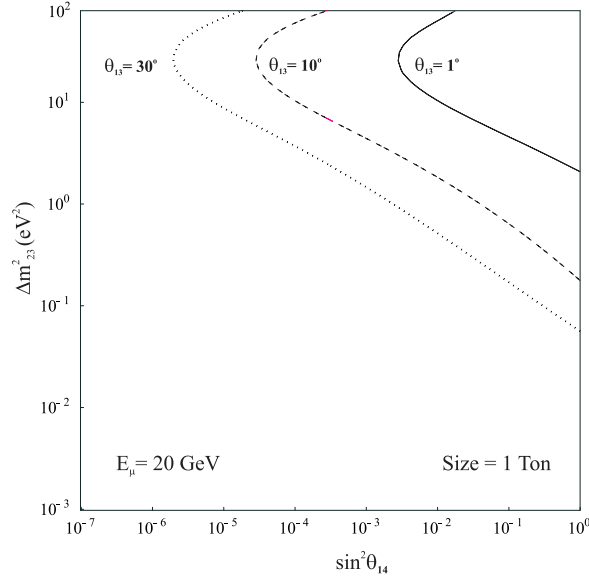


Fig. 4. Sensitivity reach in the $s_{14}^2/\Delta m_{23}^2$ plane at different values of $\theta_{13} = 1^\circ, 10^\circ$ and 30° for τ^- appearance. We consider a 1 Ton detector at 1 km from the source and 2×10^{20} useful muons/year.

τ^- channel as the relative sign between the two terms in $P(\nu_\mu \rightarrow \nu_\tau)$, eq. (10), is positive.

The overall conclusion of this analysis is that, in the minimal scheme for four-neutrino families, a 1 Ton near detector with μ and τ charge identification is suitable to fully explore the CP-even part of the parameter space.

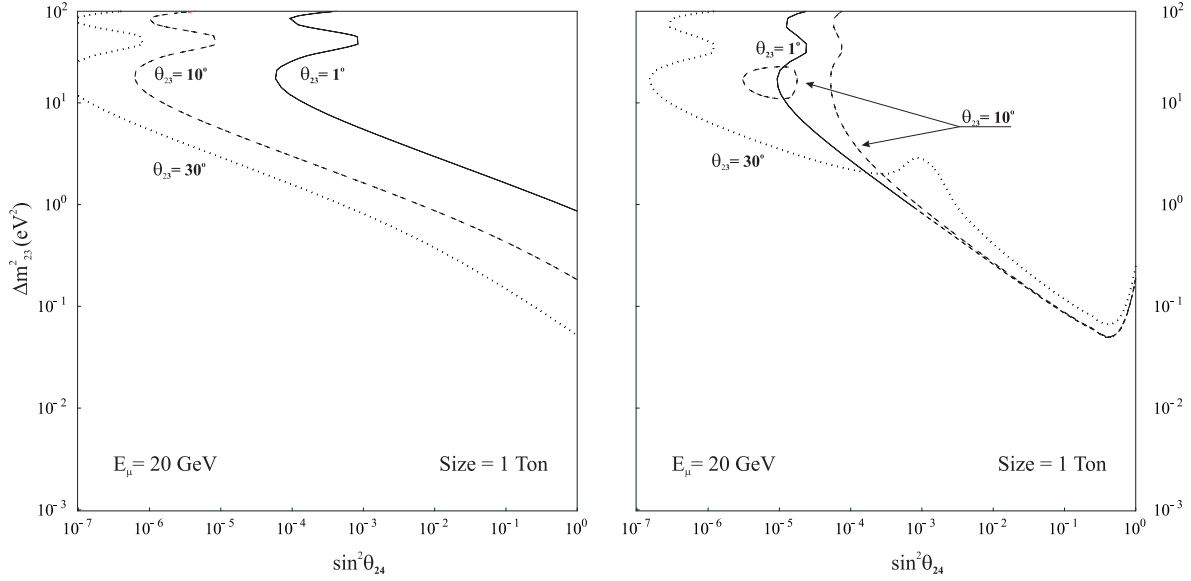


Fig. 5. Sensitivity reach in the $s_{24}^2/\Delta m_{23}^2$ plane at different values of $\theta_{23} = 1^\circ, 10^\circ$ and 30° for τ^- (left) and τ^+ (right) appearance. We consider a 1 Ton detector at 1 km from the source and 2×10^{20} useful muons/year.

2.2 CP Violation with four light neutrino species

As in the standard three-family scenario, in order to reach observable CP-odd effects in oscillations it is necessary to have both physical CP-odd phases and at least two non-vanishing mass differences. The next-to minimal or “two mass scale dominance” scheme, described at the beginning of this section, is thus suitable.

As explained above, the parameter space consists of five angles and two CP-odd phases. Expanding the transition probabilities to leading order in Δm_{atm}^2 (i.e. Δm_{34}^2 in our parametrization), it follows that their CP-odd components are³:

$$P_{\mathcal{CP}}(\nu_e \rightarrow \nu_e) = P_{\mathcal{CP}}(\nu_\mu \rightarrow \nu_\mu) = P_{\mathcal{CP}}(\nu_\tau \rightarrow \nu_\tau) = 0, \quad (13)$$

$$P_{\mathcal{CP}}(\nu_e \rightarrow \nu_\mu) = 8c_{13}^2 c_{23}^2 c_{24} c_{34} s_{24} s_{34} \sin(\delta_2 + \delta_3) \left(\frac{\Delta m_{34}^2 L}{4E_\nu} \right) \sin^2 \left(\frac{\Delta m_{23}^2 L}{4E_\nu} \right) \quad (14)$$

$$P_{\mathcal{CP}}(\nu_e \rightarrow \nu_\tau) = 4c_{23} c_{24} \left\{ 2c_{14} s_{14} c_{23} s_{23} s_{13} s_{24} (s_{13}^2 s_{14}^2 - c_{14}^2) \sin(\delta_2 + \delta_3) \right. \\ \left. + c_{14} c_{34} s_{13} s_{14} s_{34} \left[(s_{23}^2 - s_{24}^2) \sin \delta_2 + s_{23}^2 s_{24}^2 \sin(\delta_2 + 2\delta_3) \right] \right. \\ \left. + c_{14} c_{24} s_{13} s_{14} s_{23} s_{24} (c_{34}^2 - s_{34}^2) \sin \delta_3 \right\} \left(\frac{\Delta m_{34}^2 L}{4E_\nu} \right) \sin^2 \left(\frac{\Delta m_{23}^2 L}{4E_\nu} \right) \quad (15)$$

$$P_{\mathcal{CP}}(\nu_\mu \rightarrow \nu_\tau) = 8c_{13}^2 c_{23}^2 c_{24} c_{34} s_{34} \left[c_{14} c_{23} s_{13} s_{14} \sin \delta_2 + c_{14}^2 s_{23} s_{24} \sin(\delta_2 + \delta_3) \right] \times$$

³ At this order also sub-leading terms in the CP-even sector contribute. Although we do not illustrate them, all orders in Δm_{atm}^2 are included in the numerical computations.

$$\left(\frac{\Delta m_{34}^2 L}{4E}\right) \sin^2\left(\frac{\Delta m_{23}^2 L}{4E}\right). \quad (16)$$

Two distinct phases appear, δ_2 and δ_3 , in a typical sinusoidal dependence which is the trademark of CP-violation and ensures different transition rates for neutrinos and anti neutrinos.

CP-odd effects are observable in ‘‘appearance’’ channels, while ‘‘disappearance’’ ones are only sensitive to the CP-even part. The latter is mandated by CPT [18]. In contrast with the three-neutrino case, the solar suppression (see [9]) is now replaced by a less severe atmospheric suppression. CP-violating effects are then expected to be one or two orders of magnitude larger than in the standard case, and independent of the solar parameters.

Staying in the ‘‘conservative’’ assumption of small $\theta_{13}, \theta_{14}, \theta_{23}, \theta_{24}$, we compare two democratic scenarios, in which all these angles are taken to be small and of the same order:

- (1) Set 1: $\theta_{34} = 45^\circ$, $\theta_{ij} = 5^\circ$ and $\Delta m_{atm}^2 = 2.8 \times 10^{-3} \text{ eV}^2$ for $\Delta m_{LSND}^2 = 0.3 \text{ eV}^2$;
- (2) Set 2: $\theta_{34} = 45^\circ$, $\theta_{ij} = 2^\circ$ and $\Delta m_{atm}^2 = 2.8 \times 10^{-3} \text{ eV}^2$ for $\Delta m_{LSND}^2 = 1 \text{ eV}^2$.

The value chosen for Δm_{atm}^2 is the central one of the most recent SuperK analysis [1]. For illustration we consider in what follows a 1 kTon detector located at $O(10)$ km distance from the neutrino source. In the figures below, the exact formulae for the probabilities have been used.

The easiest way to measure CP-violation in oscillation is to build a CP-asymmetry or a T-asymmetry:

$$A_{\alpha\beta}^{CP} \equiv \frac{P(\nu_\alpha \rightarrow \nu_\beta) - P(\bar{\nu}_\alpha \rightarrow \bar{\nu}_\beta)}{P(\nu_\alpha \rightarrow \nu_\beta) + P(\bar{\nu}_\alpha \rightarrow \bar{\nu}_\beta)}, \quad (17)$$

$$A_{\alpha\beta}^T \equiv \frac{P(\nu_\alpha \rightarrow \nu_\beta) - P(\nu_\beta \rightarrow \nu_\alpha)}{P(\nu_\alpha \rightarrow \nu_\beta) + P(\nu_\beta \rightarrow \nu_\alpha)}. \quad (18)$$

$A_{\alpha\beta}^{CP}$ and $A_{\alpha\beta}^T$ are theoretically equivalent in vacuum due to *CPT*, and matter effects are negligible at the short distances under consideration. Their extraction from data at a *neutrino factory* is quite different, though. Consider, as an example, the $(e\mu)$ -channel. The CP-asymmetry, $A_{e\mu}^{CP}$, would be measured by first extracting $P(\nu_\mu \rightarrow \nu_e)$ from the produced (wrong-sign) μ^- s in a beam from μ^+ decay and $P(\bar{\nu}_e \rightarrow \bar{\nu}_\mu)$ from the charge conjugate beam and process. Notice that even if the fluxes are very well known, this requires a good knowledge of the cross section ratio $\sigma(\bar{\nu}_\mu \rightarrow \mu^+)/\sigma(\nu_\mu \rightarrow \mu^-)$. Conversely, the measurement of the T-asymmetry, $A_{e\mu}^T$, requires to consider $P(\nu_\mu \rightarrow \nu_e)$ and thus a good e charge identification, that seems harder to achieve. In the following we will deal only with CP-asymmetries.

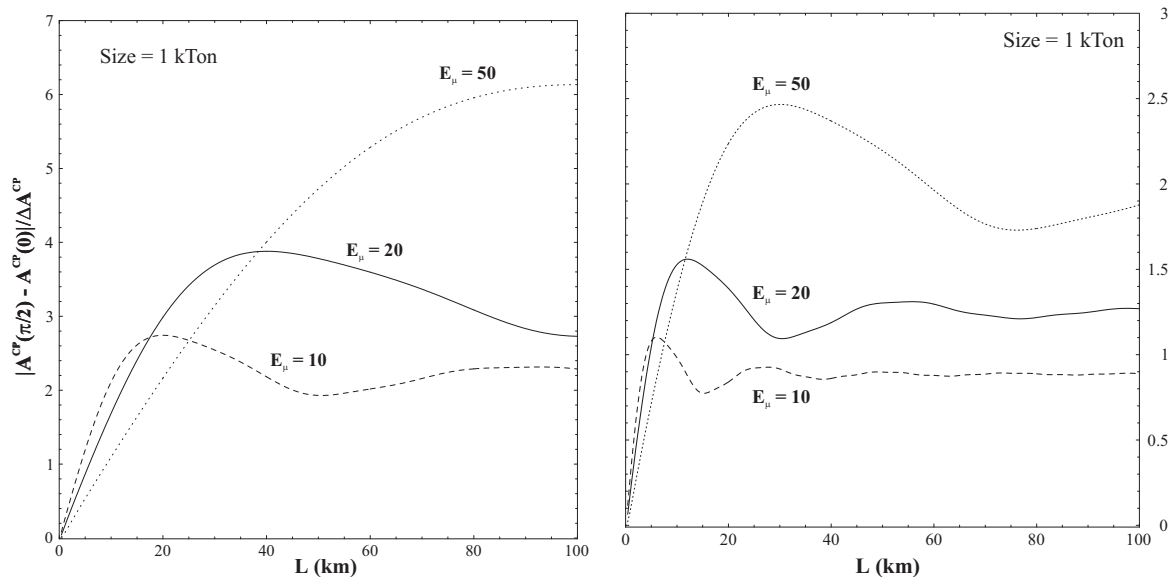


Fig. 6. *Signal over statistical uncertainty for CP violation, in the $\nu_e \rightarrow \nu_\mu$ channel, for the two sets of parameters described in the text (Set 1 on the left and Set 2 on the right). We consider a 1 kTon detector and 2×10^{20} useful muons/year.*

A central question on the observability of CP-violation is that of statistics. We do not exploit here the explicit E_ν dependence of the CP-odd effect, and we consider the neutrino-energy integrated quantity:

$$\bar{A}_{e\mu}^{CP}(\delta) = \frac{\{N[\mu^-]/N_o[e^-]\}_+ - \{N[\mu^+]/N_o[e^+]\}_-}{\{N[\mu^-]/N_o[e^-]\}_+ + \{N[\mu^+]/N_o[e^+]\}_-}, \quad (19)$$

where the sign of the decaying muons is indicated by a subindex, $N[\mu^+]$ ($N[\mu^-]$) are the measured number of wrong-sign muons, and $N_o[e^+]$ ($N_o[e^-]$) are the expected number of $\bar{\nu}_e$ (ν_e) charged current interactions in the absence of oscillations. In order to quantify the significance of the signal, we compare the value of the integrated asymmetry with its error, in which we include the statistical error and a conservative background estimate at the level of 10^{-5} .

The size of the CP-asymmetries is very different for μ channels and τ channels. For instance for Set 2, they turn out to be small in $\nu_e - \nu_\mu$ oscillations, ranging from the per mil level to a few percent. In contrast, in $\nu_\mu - \nu_\tau$ oscillations they attain much larger values of about 50% – 90%. This means that their hypothetical measurement should be rather insensitive to systematic effects, and other conventional neutrino beams from pion and kaon decay could be appropriate for their study.

- **μ appearance channels**

Fig. 6 shows the signal over noise ratio for the integrated CP asymmetry, eqs. (19), in the wrong sign muon channel, that is $\nu_e \rightarrow \nu_\mu$ versus $\bar{\nu}_e \rightarrow \bar{\nu}_\mu$ oscillations, as a function of the distance. Matter effects, although negligible, have been included. For

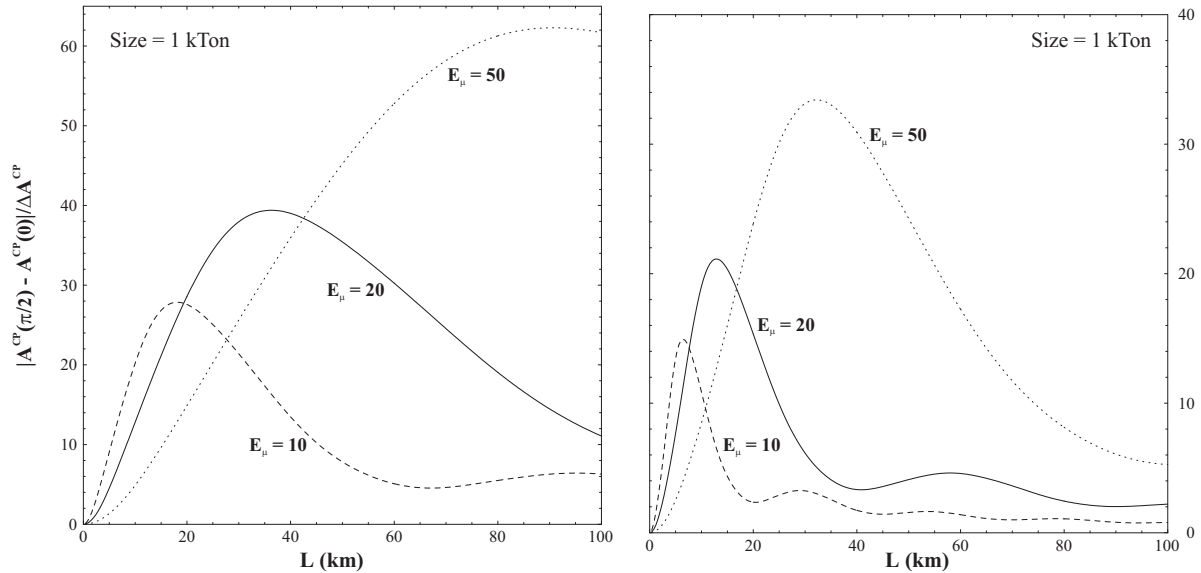


Fig. 7. Signal over statistical uncertainty for CP violation, in the $\nu_\mu \rightarrow \nu_\tau$ channel, for the two sets of parameters described in the text (Set 1 on the left and Set 2 on the right). We consider a 1 kTon detector and 2×10^{20} useful muons/year.

the scenario and distances discussed here, the scaling laws are analogous to those derived for three neutrino species in vacuum, [9,10,11], that is

$$\frac{A_{e\mu}^{CP}}{\Delta A_{e\mu}^{CP}} \propto \sqrt{E_\nu} \left| \sin \left(\frac{\Delta m_{34}^2 L}{4E_\nu} \right) \right|. \quad (20)$$

The maxima of the curves move towards larger distances when the energy of the muon beam is increased, or the assumed LSND mass difference is decreased. Moreover, increasing the energy enhances the significance of the effect at the maximum as expected. At $E_\mu = 50$ GeV, 6 standard deviation (sd) signals are attainable at around 100 km for the values in Set 1, and just 2.5 sd at 30 km for Set 2, levelling off at larger distances and finally diminishing when E_ν/L approaches the atmospheric range.

- **τ appearance channels**

In Fig. 7 we show the signal over noise ratio in $\nu_\mu \rightarrow \nu_\tau$ versus $\bar{\nu}_\mu \rightarrow \bar{\nu}_\tau$ oscillations as a function of the distance. The experimental asymmetry and the corresponding scaling law are obtained from eq. (19) and eq. (20), with the obvious replacements $e \rightarrow \mu$ and $\mu \rightarrow \tau$. A larger enhancement takes place in this channel as compared to the $\nu_e \rightarrow \nu_\mu$ one: over 60 sd for Set 1 and 33 sd for Set 2 are a priori attainable. These larger factors follow from the fact that the CP-even transition probability $P_{CP}(\nu_\mu \nu_\tau)$ is smaller than $P_{CP}(\nu_e \nu_\mu)$, due to a stronger suppression in small mixing angles. Notice that the opposite happens in the 3-species case. Bilenky *et al.* [17] had previously concluded that the τ channel was best for CP-studies in the four

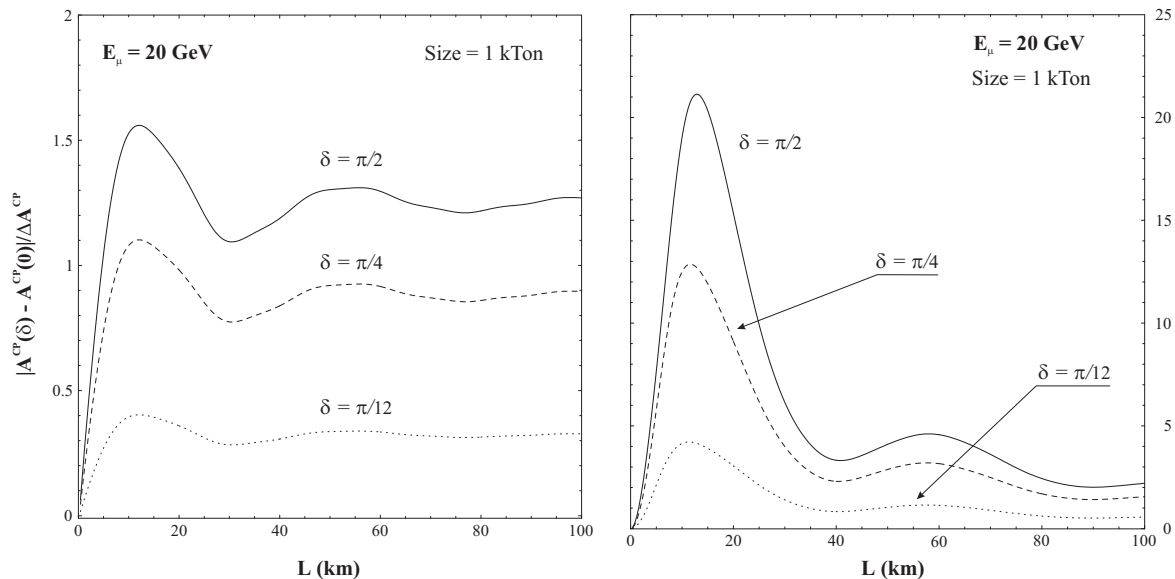


Fig. 8. *CP violation asymmetry in the $\nu_e \rightarrow \nu_\mu$ (left) and $\nu_\mu \rightarrow \nu_\tau$ (right) channel for $E_\mu = 20$ GeV, angles and mass differences as in Set 2 and for different choice of the CP phases: $\delta_1 = \delta_2 = \delta_3 = \pi/2$ (full line), $\pi/4$ (dashed line) and $\pi/12$ (dotted line). We consider a 1 kTon detector from the source of a 2×10^{20} muon/year beam.*

species scenario. Their argument relied, though, on the fact that the parameter space involved in ν_τ oscillations is experimentally less constrained than the ν_μ one, a freedom we have not used here, staying within the more natural assumption that all the angles in the next-to-minimal scheme, except the atmospheric one, θ_{34} , are small.

The results in the $\nu_e \rightarrow \nu_\tau$ channels are almost identical to the $\nu_e \rightarrow \nu_\mu$ ones, not deserving a separate discussion.

The phase dependence is shown in Fig. 8, with the expected depletion of the signal for small CP phases. For small values of the phases, i.e. $\delta_1 = \delta_2 = \delta_3 = 15^\circ$, the significance drops to the 1σ level.

3 Conclusions

The ensemble of solar, atmospheric and LSND neutrino data, are analysed in a three active plus one sterile scenario. A *neutrino factory* from muon storage beams has much higher precision and discovery potential than any other planned facility. The reach of SBL experiments is extremely large. We have derived one and two mass scale dominance approximations, appropriate for CP-even and CP-odd observables, respectively. The number of useful observables is sufficient to determine or very significantly constrain all the mixing parameters of a four-generation mixing scheme.

CP violation may be easily at reach, specially through “ τ appearance” signals. In these channels the CP-asymmetries are so large that even neutrino beams from conventional pion and kaon decays may be sufficient for their detection. Matter effects are irrelevant in the energy integrated CP-odd observables for such a short baseline, making the measure of CP-violation extremely clean in this four neutrino scenario.

4 Acknowledgements

We acknowledge useful conversations with: B. Autin, A. De Rújula, F. Dydak, J. Gómez-Cadenas, M.C. Gonzalez-Garcia, O. Mena, S. Petcov and A. Romanino. The work of A. D., M. B. G., and S. R. was partially supported by CICYT project AEN/97/1678. A. Donini acknowledges the I.N.F.N. for financial support. S. Rigolin acknowledges the European Union for financial support through contract ERBFM-BICT972474.

References

- [1] Y. Fukuda *et al.*, Phys. Lett. **B433**, (1998) 9, Phys. Rev. Lett. **81** (1998) 1562, Phys. Rev. Lett. **82**, (1999) 2644;
A. Habig, hep-ex/9903047.
- [2] B.T. Cleveland *et al.*, Astrophys. J. **496**, (1998) 505;
K.S. Hirata *et al.*, Phys. Rev. Lett. **77**, (1996) 1683;
W. Hampel *et al.*, Phys. Lett. B **388**, (1996) 384;
D.N. Abdurashitov *et al.*, Phys. Rev. Lett. **77**, (1996) 4708.
- [3] Y. Fukuda *et al.*, Phys. Rev. Lett. **81**, (1998) 1158, Phys. Rev. Lett. **82**, (1999) 2430;
M.B. Smy, hep-ex/9903034.
- [4] Y. Fukuda *et al.* Phys. Lett. B **335**, (1994) 237;
R. Becker-Szendy *et al.* Nucl. Phys. B (Proc. Suppl.) **38**, (1995) 331;
W.W.M. Allison *et al.* hep-ex/9901024;
M. Ambrosio *et al.* Phys. Lett. B **434**, (1998) 451.
- [5] C. Athanassopoulos *et al.*, Phys. Rev. Lett. **75**, (1995) 2650, Phys. Rev. Lett. **77**, (1996) 3082, Phys. Rev. Lett. **81**, (1998) 1774, Phys. Rev. C **58** (1998) 2489.
- [6] B. Pontecorvo, Sov. Phys. JETP **26** (1968) 984.
- [7] J. T. Peltoniemi and J. W. F. Valle, Nucl. Phys. **B406**, (1993) 409;
D. Caldwell and R. N. Mohapatra, Phys. Rev. **D50**, (1994) 3477;
G. M. Fuller, J. R. Primack and Y.-Z. Qian, Phys. Rev. **D52**, (1995) 1288;
J. J. Gomez-Cadenas and M. C. Gonzalez-Garcia, Zeit. Phys. **C71**, (1996) 443;

- E. Ma and P. Roy, Phys. Rev. **D52**, (1995) R4780;
 E. Ma and J. Pantaleone, Phys. Rev. **D52**, (1995) R3763;
 R. Foot and R. R. Volkas, Phys. Rev. **D52**, (1995) 6595;
 Z. G. Berezhiani and R. N. Mohapatra, Phys. Rev. **D52**, (1995) 6607;
 E. J. Chun, A. S. Joshipura and A. Y. Smirnov, Phys. Lett. **B357**, (1995) 608;
 Q. Y. Liu and A. Yu. Smirnov, hep-ph/9712493;
 V. Barger, K. Whisnant and T. Weiler, Phys. Lett. **B427**, (1998) 97;
 S. C. Gibbons, R. N. Mohapatra, S. Nandi and A. Raychaudhuri, Phys. Lett. **B430**,
 (1998) 296;
 V. Barger, Y.B. Dai, K. Whisnant and B.L. Young, hep-ph/9901388;
 D. Dooling, C. Giunti, K. Kang, C.W. Kim, hep-ph/9908513;
 A. Kalliomaki, J. Maalampi and M. Tanimoto, hep-ph/9909301.
- [8] C. Caso *et al.*, EPJ **C3** (1998), 319.
- [9] A. de Rujula, M.B. Gavela and P. Hernandez, Nucl. Phys. **B547** (1999) 21.
- [10] A. Donini, M.B. Gavela, P. Hernandez and S. Rigolin, talk given at the Nufact '99 Workshop, July 5-9th, Lyon.
- [11] A. Donini, M. B. Gavela, P. Hernandez and S. Rigolin, hep-ph/9909254.
- [12] K. Dick, M. Freund, M. Lindner and A. Romanino, hep-ph/9903308. J. Sato, hep-ph/9910442.
- [13] A. Romanino, talk given at the Nufact '99 Workshop, July 5-9th, Lyon;
 A. Romanino, hep-ph/9909425.
- [14] Nufact '99 Workshop, July 5-9th, Lyon.
- [15] A. Cervera, F. Dydak and J. Gómez-Cadenas, Nufact '99 Workshop, July 5-9th, Lyon.
- [16] S. Geer, Phys. Rev **D57** (1989) 6989. B. Autin *et al.*, CERN-SPSC/98-30, SPSC/M 617 (October 1998).
- [17] S. M. Bilenky, C. Giunti and W. Grimus, Phys. Rev. **D58** (1998) 033001;
 S.M. Bilenky, C. Giunti, hep-ph/9905246;
 S.M. Bilenky *et al.*, hep-ph/9903454, hep-ph/9906251. A recent four species analysis for long baseline experiments can be found in ref. [12].
- [18] J. Bernabéu, hep-ph/9904474.